

# PHYSICAL REVIEW D

## PARTICLES AND FIELDS

THIRD SERIES, VOL. 5, NO. 5

1 March 1972

### $K^+K^-\pi^+\pi^-$ and $K^+K^-\pi^+\pi^-\pi^0$ Final States in $\bar{p}p$ Annihilations at 2.2 GeV/c\*

N. Kwak, G. H. Mall, J. E. Manweiler, and R. Stump

*Department of Physics and Astronomy, University of Kansas, Lawrence, Kansas 66044*

(Received 10 August 1971)

Approximately 7200 four-prong annihilations of 2.2-GeV/c antiprotons in hydrogen were measured. About 200 of the events contained charged kaon pairs. The cross sections for the final states  $K^+K^-\pi^+\pi^-$  and  $K^+K^-\pi^+\pi^-\pi^0$  were measured as  $192 \pm 26$  and  $488 \pm 50$   $\mu\text{b}$ , respectively. The main feature of the reactions is the production of  $K^*(890)$ ,  $\rho(760)$ , and  $\omega(783)$ .

Recently, extensive searches for direct-channel resonances in the antiproton-annihilation reactions have been conducted.<sup>1,2</sup> A resonance structure at 2350 MeV in the  $K^+K^-\omega$  channel has been reported.<sup>2</sup> This paper deals with the resonance production in four-prong events involving two charged kaons from 2.2-GeV/c antiproton annihilation observed in the BNL 31 in. hydrogen bubble chamber.

The events came from a study of four-prong topology in about 20 000 frames of a subsample. About 7200 four-prong events were processed using TVGP and SQUAW programs. The following reactions were studied:

$$\bar{p}p \rightarrow K^+K^-\pi^+\pi^- \quad (60 \text{ events}), \quad (1)$$

$$\bar{p}p \rightarrow K^+K^-\pi^+\pi^-\pi^0 \quad (153 \text{ events}). \quad (2)$$

The majority of the events were fit to the hypotheses  $\pi^+\pi^-\pi^+\pi^-$  and  $\pi^+\pi^-\pi^+\pi^-\pi^0$  ( $\chi^2$  probability  $> 1\%$ ). A preliminary result of the four- and five-pion states was reported elsewhere.<sup>3</sup> Approximately 20% of the processed events gave acceptable kinematic fits to the hypothesis  $K^{\pm}K_1^0\pi^+\pi^-\pi^{\mp}$  in addition to reactions (1) and (2). There was no ambiguity between the four-pion hypothesis [four constraints (4C)] and the kaon hypotheses. Similarly, the events of reaction (1) were unambiguous since they fitted uniquely in 90% of the cases and the ambiguities were resolved by ionization without difficulty.

About 5% of five-pion hypotheses (1C) gave fits to kaon hypotheses. For these fits to kaon hypotheses, the ionization of tracks was carefully examined on the measuring projector by a physicist. Approximately 80% of the kaon fits were rejected by this ionization check. Most of the rejected events probably belong to the pion final states with more than one missing pion.

To select the final sample, the following requirements were imposed in addition to the usual beam-momentum and fiducial-volume cuts: (1) The  $\chi^2$  probability of the fit must be greater than 10%; (2) the missing mass squared must lie between  $-0.06$  and  $+0.08$   $\text{GeV}^2$ .

The  $\chi^2$ -probability distributions for the two reactions are essentially uniform. Figure 1 shows the distribution of missing mass squared for those events that were fitted to reaction (2). The cross sections for the two reactions are  $192 \pm 26$  and  $488 \pm 50$   $\mu\text{b}$ , respectively. Within the limited statistics the cross section for reaction (2) is in agreement with the value of  $503 \pm 71$   $\mu\text{b}$  given by the Michigan Group.<sup>2</sup>

Figure 2 shows two-body effective-mass distributions for reaction (1). The dominant feature of this reaction is a copious production of the  $K^*(890)$ . In addition, the  $\rho(760)$  and possibly  $\phi(1019)$  signals are visible.

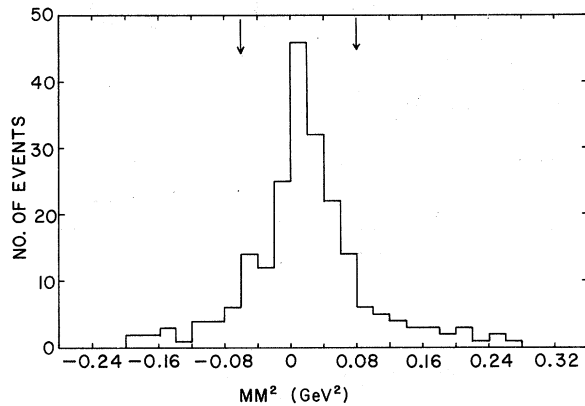
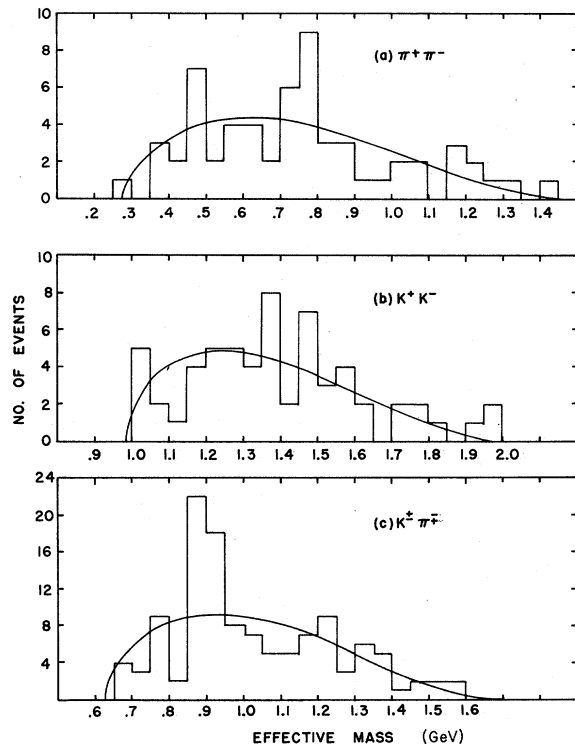
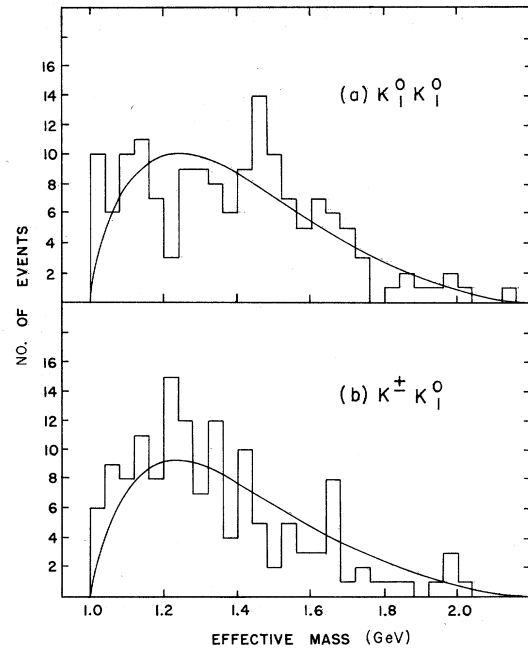


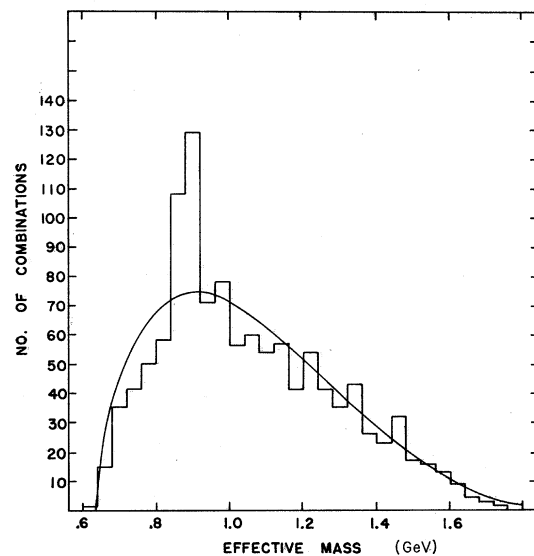
FIG. 1. Missing mass squared for the fits to reaction (2).

The distributions of  $K^+K^-$  and  $K\pi$  effective mass, which are shown in Figs. 3 and 4, respectively, are for the final states  $K_1^0 K_1^0 \pi^+ \pi^-$  and  $K_1^0 K^\pm \pi^\mp \pi^0$ , and are compared with the reaction (1). The result of analysis for those final states which contain at least a visible  $K_1^0$  has been reported previously.<sup>4</sup> One observes that the  $K^+K^-$  and  $K_1^0 K_1^0$  effective-mass distributions are essentially similar. In particular, an enhancement around 1500 MeV is noticeable, while the  $K^\pm K_1^0$  effective-mass distri-

FIG. 2. Two-body effective-mass distributions for reaction (1). (a)  $\pi^+\pi^-$ , (b)  $K^+K^-$ , (c)  $K^+\pi^-$ . The curves are phase-space predictions normalized to total events or combinations.FIG. 3. Effective-mass distributions of  $K\bar{K}$  for the final states (a)  $K_1^0 K_1^0 \pi^+ \pi^-$  (153 events) and (b)  $K^\pm K_1^0 \pi^\mp \pi^0$  (139 events). The curves are phase-space predictions.

bution indicates an excess of events around 1200 MeV. The effective-mass distribution for all combinations of  $I = \frac{1}{2} K\pi$  reveals a strong  $K^*(890)$  signal as shown in Fig. 4.

The fractions of resonance production were estimated by an incoherent sum of the  $K^*(890)$  and  $\rho(760)$ , and phase space. The resonances have been parametrized as Breit-Wigner shapes using

FIG. 4. Effective-mass distribution of  $I = \frac{1}{2} K\pi$  combinations in the final states  $K_1^0 K_1^0 \pi^+ \pi^-$  and  $K_1^0 K^\pm \pi^\mp \pi^0$ . The curve is the phase-space prediction.

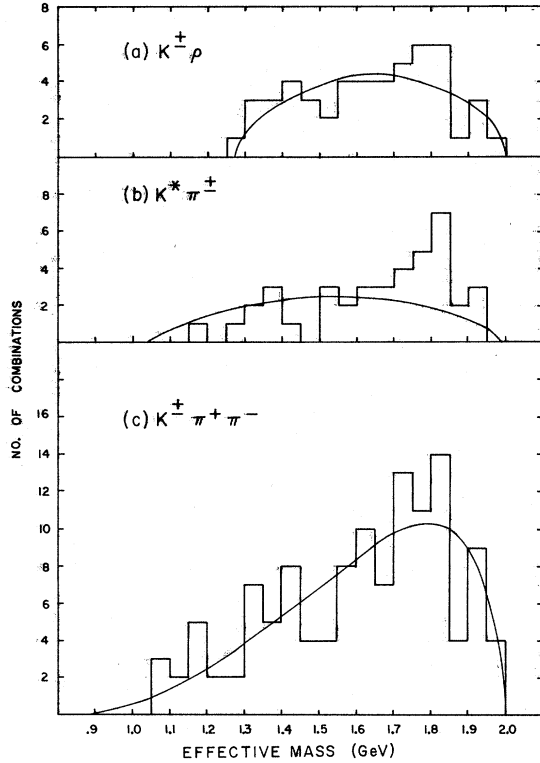


FIG. 5. Effective-mass distributions of (a)  $K^+\rho$  (640–890 MeV), (b)  $K^*(850-950 \text{ MeV})\pi^+$ , and (c)  $K^+\pi^+\pi^-$ . The curves are phase-space predictions normalized to the total combination.

the well-established masses and widths.<sup>5</sup> A Monte Carlo program was utilized to search for the maximum-likelihood fit by varying the fraction of resonances as free parameters. The total  $\chi^2$  of the fit for reaction (1) is 51.7 for 57 bins used. Table I summarizes the resonance productions for reaction (1) and the final states  $K_1^0 K_1^0 \pi^+ \pi^-$  and  $K_1^0 K^\pm \pi^\mp \pi^0$ .

There is no indication of simultaneously produced double  $K^*(890)$ 's. Apparently the absence of double- $K^*$  production in antiproton-annihilation reactions is a common characteristic throughout a wide range of energy. The effective-mass distribution of  $KK\pi$  (not shown) reveals no resonance production, however the effective-mass  $K^*(890)\pi$  distribution suggests an enhancement at about 1800 GeV as indicated in Fig. 5. A similar situation, which can be seen in Fig. 6, prevails in the final states  $K_1^0 K_1^0 \pi^+ \pi^-$  and  $K_1^0 K^\pm \pi^\mp \pi^0$ . Perhaps this  $K^*(890)\pi$  at 1800 GeV could be related to the

TABLE I. Resonance fraction for four-body final states.

Reaction	$K^*(890)$	$\rho(760)$
$\bar{p}p \rightarrow K^+K^-\pi^+\pi^-$	$70 \pm 10$	$20 \pm 5$
$\rightarrow K_1^0 K_1^0 \pi^+ \pi^-$	$45 \pm 10$	$8 \pm 5$
$\rightarrow K^\pm K_1^0 \pi^\mp \pi^0$	$35 \pm 10$	$12 \pm 5$

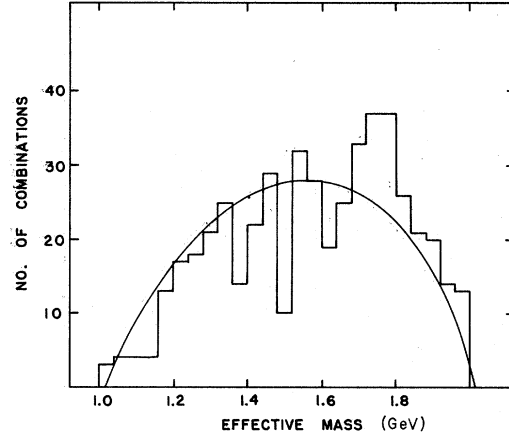


FIG. 6. Effective-mass distribution of  $K^*(850 < M_{K^*} < 925 \text{ MeV})\pi^+$  in the final states  $K_1^0 K_1^0 \pi^+ \pi^-$  and  $K_1^0 K^+ \pi^+ \pi^0$ . The curve is the phase-space prediction.

$L(1775)$  meson.

The distributions of two- and three-body effective masses for reaction (2) are presented in Figs. 7 and 8. There is no apparent  $\rho(760)$  signal but there is a moderate  $\omega(783)$  signal. The size of the  $\omega(783)$  signal seems to be comparable to those observed at lower energies.<sup>2,6</sup> A strong  $K^*(890)$  is evident

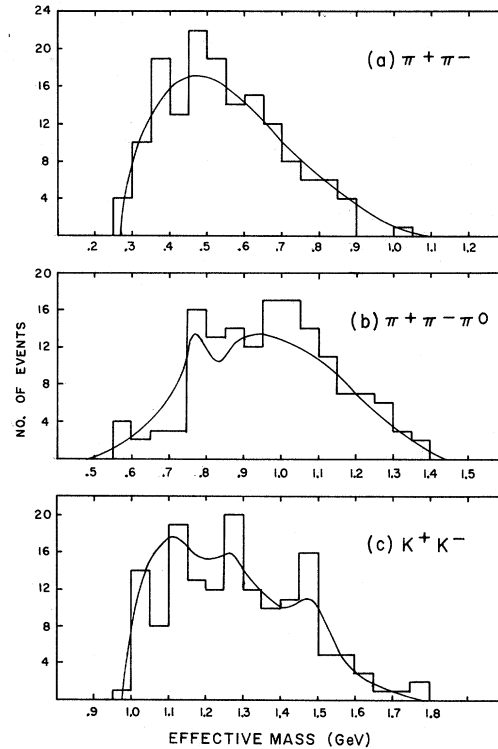


FIG. 7. Effective-mass distributions for (a)  $\pi^+\pi^-$ , (b)  $\pi^+\pi^-\pi^0$ , and (c)  $K^+K^-$  of reaction (2). The curves are predictions of incoherent sum of  $K^*(890)$ ,  $\omega(783)$ ,  $K^+K^-(1500)$ , and  $A_2(1280)$ , and phase space as described in text.

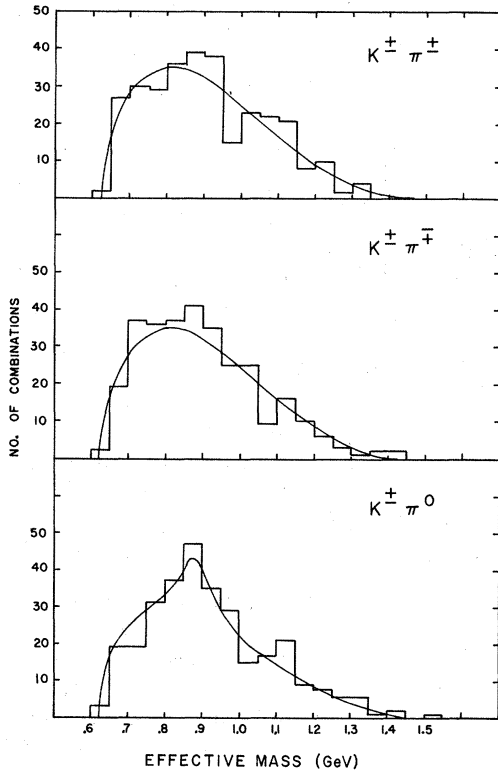


FIG. 8.  $K\pi$  effective-mass distributions in various charged modes for reaction (2). The curves are defined as in Fig. 7.

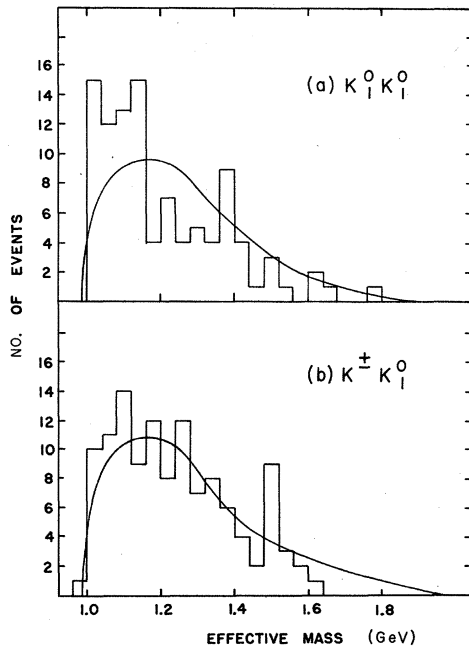


FIG. 9. Effective-mass distribution of  $KK$  for the final states (a)  $K_1^0 K_1^0 \pi^+ \pi^- \pi^0$  (103 events) and (b)  $K_1^0 K_1^0 \pi^+ \pi^- \pi^+$  (120 events). The curves are phase-space predictions.

only in the singly charged state. The final state  $K_1^0 K_1^+ \pi^+ \pi^- \pi^0$  has a similar  $K^+ K_1^0$  effective-mass distribution to the  $K^+ K^-$  distribution for reaction (2) as shown in Fig. 9. On the other hand the final state  $K_1^0 K_1^0 \pi^+ \pi^- \pi^0$  shows a somewhat different distribution. Namely, there is an indication of  $\phi(1019)$  production and an excess of events at  $K\bar{K}$  threshold.

Table II presents the resonance production in the final states  $K_1^0 K_1^0 \pi^+ \pi^- \pi^0$  and  $K_1^0 K_1^+ \pi^+ \pi^- \pi^0$  in addition to reaction (2) assuming only the production of the  $K^*(890)$ ,  $\rho(760)$ , and  $\omega(783)$ , plus phase space.

One remark for reaction (2) is worthwhile mentioning. The resulting total  $\chi^2$  (114 for 95 bins) of the fit which is presented in Table II indicates by no means the best fit. Indeed the fit was significantly improved by adding a  $K^+ K^-$  enhancement at 1500 MeV, and gave the total  $\chi^2$  of 93 for 95 bins used. The best set of resonance fractions are 24%  $K^*$ , 30%  $\omega$ , 30%  $K^+ K^-$  (~1500) enhancement, and 5%  $A_2(1280)$ . The  $K^+ K^-$  (~1500) enhancement was parametrized as  $m(K^+ K^-) = 1500$  MeV,  $\Gamma(K^+ K^-) = 70$  MeV. The predictions of this fit are given by solid curves in Figs. 7 and 8. Of course, the enhancement around 1500 MeV requires further studies and a firm confirmation. Until then one should not take seriously the result of the best fit.

The three-body effective masses of  $KK\pi$  and  $K\pi\pi$  for reaction (2) are practically featureless. Figure 10 is an effective-mass scatter diagram of  $K^\pm \pi^\mp$  and  $K^\mp \pi^0$ , which shows a slight enhancement of points in the  $K^*(890)$  overlapping region. This suggests that a quasi-three-body process such as  $K^{*0} K^{*\pm} \pi^\mp$  does occur to some extent. A similar study of a scatter diagram of  $K^+ \pi^-$  against  $K^- \pi^+$  effective mass does not indicate any substantial evidence of a quasi-three-body  $K^{*0} K^{*0} \pi^0$  process.

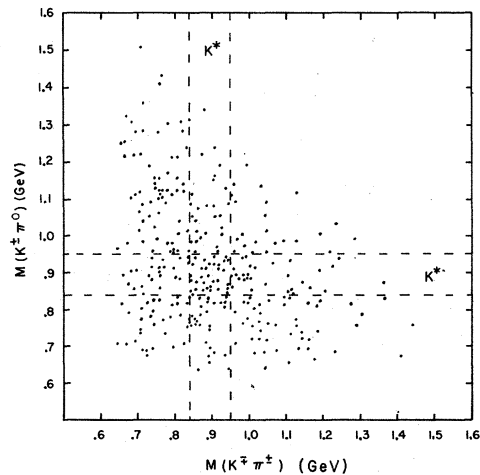


FIG. 10. A scatter diagram of the  $K^\pm \pi^\mp$  effective mass vs the  $K^\mp \pi^0$  effective mass in reaction (2).

TABLE II. Resonance fraction for five-body final states.

Reaction	$K^*(890)$	$\rho(760)$	$\omega(783)$
$\bar{p}p \rightarrow K^+K^-\pi^+\pi^-\pi^0$	$40 \pm 5$	0	$30 \pm 5$
$\rightarrow K_1^0 K_1^0 \pi^+ \pi^- \pi^0$	$43 \pm 15$	$20 \pm 10$	$10 \pm 5$
$\rightarrow K^{\pm} K_1^0 \pi^{\mp} \pi^+ \pi^-$	$60 \pm 15$	$11 \pm 7$	...

In conclusion, the  $K^*(890)$ ,  $\rho(760)$  and  $K^*(890)$ ,  $\omega(783)$  productions are the dominant feature of reactions (1) and (2), respectively. There is no indication of  $D(1285)$  or  $K_A(1250)$  either. Quasi-two-body processes are almost completely absent, while three-body processes occur to some extent. The final state  $K^+K^-\omega$  amounts to about 30% of reaction (2).

\*Work supported in part by the National Science Foundation.

<sup>1</sup>B. Y. Oh, D. L. Parker, P. S. Eastman, G. A. Smith, R. J. Sprafka, and Z. M. Ma, Phys. Rev. Letters 24, 1257 (1970); J. Lys, J. W. Chapman, D. G. Falconer, C. T. Murphy, and J. C. Vander Velde, *ibid.* 21, 1116 (1968); J. W. Chapman, F. Hess, J. Lys, C. T. Murphy, and J. C. Vander Velde, *ibid.* 21, 1718 (1968); J. W. Chapman, J. Davidson, R. Green, J. Lys, B. Roe, and J. C. Vander Velde, Nucl. Phys. B24, 445 (1970); J. K. Yoh, B. C. Barish, N. Nicholson, J. Pine, A. V. Tollestrup, A. S. Carroll, R. H. Phillips, D. Delorme, F. Lobkowicz, A. C. Melissinos, and Y. Nagashima, Phys. Rev. Letters 23, 506 (1969).

<sup>2</sup>J. W. Chapman, R. Green, J. Lys, C. T. Murphy, H. M. Ring, and J. C. Vander Velde, Phys. Rev. D 4, 1275 (1971).

<sup>3</sup>N. Kwak, G. H. Mall, J. E. Manweiler, T. A. Stringer, and R. Stump, Bull. Am. Phys. Soc. 15, 29 (1970).

<sup>4</sup>R. Stump, N. Kwak, J. Manweiler, G. Mall, and T. Stringer, in *Proceedings of the Fourteenth International Conference on High Energy Physics, Vienna, 1968*, edited by J. Prentki and J. Steinberger (CERN, Geneva, Switzerland, 1968), p. 492.

<sup>5</sup>Particle Data Group, Phys. Letters 33B, 1 (1970).

<sup>6</sup>A. G. Frodesen, O. Skjeggstad, R. S. Moore, and S. Reucraft, Nucl. Phys. B10, 307 (1969).

## Measurement of $\Lambda^0$ Mass\*

L. G. Hyman, K. O. Bunnell,† M. Derrick, T. Fields, P. Katz,‡ and G. Keyes§  
Argonne National Laboratory, Argonne, Illinois 60439

and

J. G. Fetkovich, J. McKenzie,|| and I-T. Wang\*\*  
Carnegie-Mellon University, Pittsburgh, Pennsylvania 15213

(Received 27 October 1971)

Using  $\Lambda$  hyperons produced by negative kaons in a helium bubble chamber, we have measured the  $\Lambda^0$  mass to be  $M_{\Lambda^0} = 1115.59 \pm 0.08 \text{ MeV}/c^2$ . This result is based mainly on curvature and angle measurements of the proton and  $\pi^-$  tracks from the  $\Lambda$  decay.

### I. INTRODUCTION

Both emulsion and bubble-chamber experiments have provided useful data on hyperon masses.<sup>1,2</sup> The two techniques are somewhat complementary, with emulsions offering high spatial precision and a well-studied range-energy relation, whereas bubble-chamber data are usually characterized by small multiple Coulomb scattering, precise magnetic curvature information ( $\Delta p/p \sim 1\%$  on a single track), and the availability of kinematic information from the production reaction.

In the present experiment we have used helium-bubble-chamber pictures to obtain a measurement of the  $\Lambda^0$  mass. Considerable effort was made to

accurately establish the range-energy relation for helium,<sup>3,4</sup> as well as to achieve high spatial precision. In addition, the magnetic field (provided by a superconducting magnet) was measured<sup>3</sup> to an accuracy of  $\pm 0.1\%$ . Thus, the experiment possesses some of the advantages of both emulsion and bubble-chamber techniques.

### II. DESCRIPTION OF EXPERIMENT

#### A. General Procedure

To measure the  $\Lambda^0$  mass we studied reactions of the types